

Coherent control of photon transmission: Slowing light in a coupled resonator waveguide doped with Λ atoms

Lan Zhou

*Department of Physics, Hunan Normal University, Changsha 410081, China
and Institute of Theoretical Physics, Chinese Academy of Sciences, Beijing, 100080, China*

Jing Lu

Department of Physics, Hunan Normal University, Changsha 410081, China

C. P. Sun*

Institute of Theoretical Physics, Chinese Academy of Sciences, Beijing 100080, China

(Received 23 November 2006; published 16 July 2007; corrected 23 July 2007)

In this paper, we propose and study a hybrid mechanism for coherent transmission of photons in the coupled resonator optical waveguide (CROW) by incorporating the electromagnetically induced transparency (EIT) effect into the controllable band gap structure of the CROW. Here, the configuration setup of system consists of a CROW with homogeneous couplings and the artificial atoms with Λ -type three levels doped in each cavity. The roles of three levels are completely considered based on a mean field approach where the collection of three-level atoms collectively behave as two-mode spin waves. We show that the dynamics of low excitations of atomic ensemble can be effectively described by a coupling boson model. The exact solutions show that the light pulses can be stopped and stored coherently by adiabatically controlling the classical field.

DOI: 10.1103/PhysRevA.76.012313

PACS number(s): 42.50.Pq, 03.67.-a, 42.70.Qs, 73.20.Mf

I. INTRODUCTION

Electromagnetically induced transparency (EIT) is a phenomenon that usually occurs for atomic ensemble as an active mechanism to slow down or stop laser pulse completely [1–4]. Usually, the EIT effect happens in the so-called Λ -type atomic system, which contains two lower states with separate couplings to an excited state via two electromagnetic fields (probe and control light). When the absorption on both transitions is suppressed due to destructive interference between excitation pathways to the upper level, the medium becomes transparent with respect to the probe field.

Most recently, an EIT-like effect has been displayed in the experiment via all optical on-chip setups with the coupled resonator optical waveguide (CROW) [5,6]. The bare CROW for photons behaves as the tight-binding lattice with band structure for electrons; thus, the CROW forms a new type of photonic crystal. It was discovered that, by coupling each resonator in the CROW to an extra cavity, the resonant spectral line is shifted and the band width is compressed, thus the propagating of light pulses is stopped and the information carried by light is stored [7–9]. The scheme of stopping, storing, and releasing light is also theoretically proposed and analyzed for quantum-well Bragg structures, which form a one-dimensional resonant photonic band-gap structure [10].

Actually, with the help of modern nanofabrication technology, the hybrid structure, i.e., an array of coupled cavities with doping artificial atoms can be implemented experimentally with a photonic crystal or other semiconductor systems. By making use of such a hybrid system [11,12], a Mott insulator and superfluid state can emerge in different phases of the polaritons formed by dressing the doping atoms with the gapped light field. Also the hybrid system of a two-dimensional array of coupled optical cavities in the photon-blockade regime will undergo a characteristic Mott insulator (excitations localized on each site) to superfluid (excitations delocalized across the lattice) quantum phase transition [13]. Such a coplanar hybrid structure based on a superconducting circuit, has been proposed by us [14] for the coherent control of microwave photons propagating in a coupled superconducting transmission line resonator (CTLR) waveguide [15,16].

By making use of the two time Green function approach, we studied the coherent control of photon transmission along the homogeneous CROW by doping two-level atoms [17]. Usually, to realize the controllable and robust two-level system, a three-level atom is used to reduce an effective two-level structure through the stimulated Raman mechanism, which is a two-photon process decoupling the two direct transitions to an upper energy level in the case with large detuning. Then the induced coupling between two lower energy levels can be obtained by the adiabatic elimination of the upper energy level.

In this paper, we study the photon transmission in a homogeneous CROW controlled coherently by doped three-level Λ -type systems, where the upper energy level is not eliminated adiabatically. To consider the coherent roles of three energy levels directly, we use the mean field approach to deal with the collective excitations of all spatially distributed Λ -type atoms as two independent bosonic modes of quasispin waves [18]. These quasispin waves, due to interacting with the cavity modes in CROW, can change the photonic band structure of CROW so that the dispersion relation exhibits some exotic feature—a slow (and even zero veloc-

ity) feature.

*suncp@itp.ac.cn; URL: <http://www.itp.ac.cn/~suncp>

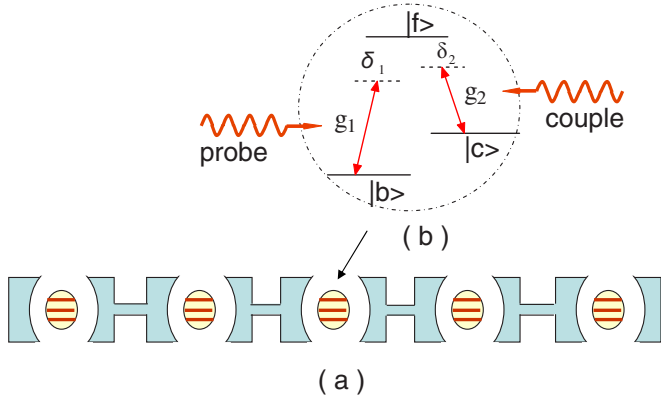


FIG. 1. (Color online) Illustrative configuration for controlling light propagation in a coupled resonators waveguide by doping atom systems: (a) A schematic of the coupled resonator optical waveguide (CROW) doped by three-level systems. The CROW can be realized as an array of periodic defects in the photonic band-gap materials, or a waveguide with coupled superconducting transmission line resonators. (b) The doping three-level atoms interacting with quantized probe light and the classical couple light. The artificial atoms can be realized as the quantum dot, or the charge and flux qubits.

ity) light pulse can emerge by some appropriate coherent control of light-atom couplings.

This paper is organized as follows: In Sec. II, we describe our model—the homogeneous CROW with each cavity doping a Λ -type three-level atom. By the mean field approach in terms of spin wave excitations, in Sec. III, we derive the effective Hamiltonian for the hybrid structure. In Sec. IV, we diagonalize the effective Hamiltonian to determine eigenfrequencies of this hybrid photon-atom system: The quasiparticles—polaritons are introduced to describe the excitations of this system. Then, in Sec. V, we discuss how the doping atoms modify the band structure of the CROW, and show how to store the information of incident pulse by adjusting the intensity of the control radiation in EIT. The absorption and dispersion of the atomic medium to the slow light pulses are studied in Sec. VI. We make our conclusion and give remarks in Sec. VII.

II. MODEL SETUP AND MOTIVATIONS

The hybrid system that we considered is shown in Fig. 1. This system consists of N single-mode cavities with homogeneous nearest-neighbor interactions, which form a one-dimensional array of cavities. Each single-mode cavity has the same resonance frequencies ω_0 . There are three practical systems to implement such an array of cavities [19]: (1) a periodic array of coupled Fabry-Pèrot cavities; (2) the coupled microdisk or microring resonators; and (3) the coupled defect modes in photonic crystals, where the band-gap cavities are formed when the periodicity of the photonic crystal is broken periodically [20,21]. The intercavity photon hopping is due to the evanescent coupling pathways between the cavities. In the coupled Fabry-Pèrot cavities and the microdisk or microring resonators, the doped system can be the

natural atom. For photonic crystals, the photonic band-gap material is fabricated in diamond; the doping systems can be realized as some ion-implanted NV centers [13]. Another promising candidate for electromagnetically controlled quantum device is based on a superconducting circuit [14], where the CROW is realized by the superconducting waveguide with coupled transmission line resonators [15,16], while the doping systems are implemented by the biased Cooper pair boxes (CPBs) (or called charge qubits), or the current biased flux qubits.

Generally, we use a_j^\dagger (a_j) to denote its creation (annihilation) operator of the j th cavity. In each cavity, the two lower levels $|b\rangle$ and $|c\rangle$ are excited to the upper level $|f\rangle$ by the quantized field and the coupling field, respectively. The energy level spacing between the upper level $|f\rangle$ and the ground state $|b\rangle$ is denoted by $\omega_{fb} = \omega_f - \omega_b$. This two-level atomic transition couples to quantized radiation modes of the waveguide cavities with coupling constant g_1 . The energy difference between the upper level $|f\rangle$ and the metastable lower state $|c\rangle$ is denoted by $\omega_{fc} = \omega_f - \omega_c$. The atomic transition from $|f\rangle$ to $|c\rangle$ is driven homogeneously by a classical field of frequency Ω with coupling constant g_2 .

Let J be the nearest-neighbor evanescent coupling constant of intercavity. The model Hamiltonian $H = H_C + H_A + H_{AC}$ consists of three parts, the cavity part with intercavity photon hoppings,

$$H_C = \sum_j^N \omega_0 a_j^\dagger a_j + J \sum_{j=1}^N a_j^\dagger a_{j+1} + \text{H.c.}, \quad (1)$$

the free atom part,

$$H_A = \sum_j^N (\omega_f \sigma_{ff}^j + \omega_b \sigma_{bb}^j + \omega_c \sigma_{cc}^j), \quad (2)$$

and the localized photon-atom interaction part,

$$H_{AC} = \sum_j^N (g_1 \sigma_{fb}^j a_j + g_2 e^{-i\Omega t} \sigma_{fc}^j + \text{H.c.}). \quad (3)$$

Here, the quasispin operators $\sigma_{\alpha\beta}^j = |\alpha\rangle_j \langle\beta|$ ($\alpha, \beta = f, b, c$) for $\alpha \neq \beta$ describe the atomic transitions among the energy levels of $|f\rangle$, $|b\rangle$, and $|c\rangle$. In practical experiments, coupling constants g_i and J depend on the positions of atoms. In this paper, we take uniform g and J for simplicity. Actually, a small difference of couplings is unavoidable in the practical implementation of the present setup, but there should be no principle difficulty in modern fabrication technique to achieve quasiuniform coupling [23]. Theoretically, the small fluctuations of coupling constants are innocuous and do not change the results of this paper qualitatively.

To illustrate our motivation using this complex hybrid structure, we may recall the fundamental principle for the EIT phenomenon briefly. Usually, an absorption region occurs to a weak probe light when it passes through a medium, but in the presence of the control light, a transparency “window” appears in the probe absorption spectrum. Here the probe light is not of single color since the photon propagating in the CROW has a photonic band. To consider whether or not EIT phenomenon emerges in this band-gap structure,

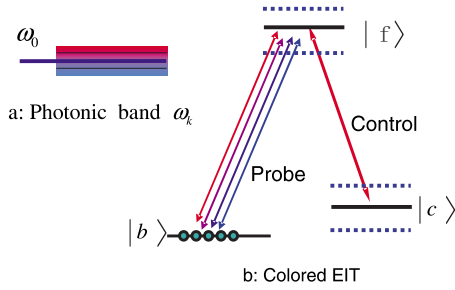


FIG. 2. (Color online) Electromagnetically induced transparency (EIT) effect in the coupled resonator optical waveguide (CROW) with photonic band structure. The problem is equivalent to that of a multimode optical pulse with different color component couples between two energy levels near resonantly. The strong light split the bare energy levels. The EIT phenomenon emerges when the band structure can match these splits. This mechanism can well control light propagation in the CROW by doping a three-level system.

we should match the photonic band structure with the splits of the energy level spacing between $|f\rangle$ and $|c\rangle$ (see Fig. 2).

As for this hybrid structure with EIT effect, it is well known that, among varieties of theoretical treatments of EIT, an approach for EIT is the “dressed state” picture, wherein the Hamiltonian of the system plus the light field is diagonalized firstly to give rise to an Autler-Townes type splitting [24] in the strong coupling limit with the control field. Then the Fano-type interference [25] between the dressed states results in EIT. Between the doublet peaks of the absorption line, a transparency window emerges as the quantum probability amplitudes for transitions to the two lower states interference. In the CROW, the emitted and absorbed photons can also be constrained by the photonic band structure. Here, the single- and two-photon resonances in EIT for a given Autler-Townes-type splitting should be reconsidered to match the band structure of the CROW. Particularly, we need to generalize the polariton approach to describe the stopped and stored light schemes. Here, the photons of the probe beam only within the photonic band can be coherently “transformed” into “dark state polaritons,” which are the dressed excitations of atom ensemble.

III. COLLECTIVE EXCITATIONS WITH ELECTROMAGNETICALLY INDUCED TRANSPARENCY EFFECT

In order to study the novel EIT effect in the CROW, we use the mean field approach that we developed for the collective excitation of an atomic ensemble with an ordered initial state [26]. This approach for EIT can be understood as a fully quantum theory, which not only gives these results about slow light propagation that can be given by a semiclassical approach, but also emphasizes the quantum states of the photon and the atomic collective excitations—quasispin waves, which are crucial for quantum information processing, such as quantum memory or storage.

Let ℓ be the distance between the nearest-neighbor cavities. The Fourier transformation

$$A_k = \frac{1}{\sqrt{N}} \sum_j \sigma_{bf}^j \exp(ik\ell j), \quad (4)$$

$$C_k = \frac{1}{\sqrt{N}} \sum_j \sigma_{bc}^j \exp(ik\ell j), \quad (5)$$

and its conjugate $A_k = (A_k^\dagger)^\dagger$, $C_k = (C_k^\dagger)^\dagger$ define the bosonlike operators to describe the collective excitation from $|b\rangle$ to $|f\rangle$ and from $|b\rangle$ to $|c\rangle$, respectively. In the large N limit, and under the low excitation condition that there are only a few atoms occupying $|f\rangle$ or $|c\rangle$, the quasi-spin-wave excitations behave as bosons since they satisfy the bosonic commutation relations

$$[A_k, A_k^\dagger] = 1, \quad [C_k, C_k^\dagger] = 1,$$

$$[A_k, C_k] = 0,$$

$$[A_k, C_k^\dagger] = -\frac{T_-}{N} \rightarrow 0. \quad (6)$$

Thus, these quasi-spin-wave low excitations are independent of each other. Here, the collective operators

$$T_- = \sum_j^N \sigma_{cf}^j, \quad T_+ = (T_-)^\dagger, \quad (7)$$

$$T_3 = \frac{1}{2} \sum_j (\sigma_{ff}^j - \sigma_{cc}^j), \quad (8)$$

generate the SU(2) algebra.

In a rotating frame with respect to the zeroth-order Hamiltonian

$$H_0 = \sum_j^N (\omega_0 a_j^\dagger a_j + \omega_f' \sigma_{ff}^j + \omega_b \sigma_{bb}^j + \omega_c \sigma_{cc}^j),$$

we achieve the coupling boson mode with the model Hamiltonian $H = \sum_k H_k$,

$$H_k = \delta_2 A_k^\dagger A_k + \Omega_k a_k^\dagger a_k + g_1 A_k^\dagger a_k + g_2 A_k^\dagger C_k + \text{H.c.}, \quad (9)$$

where we have used the Fourier transformation

$$\hat{a}_k = \frac{1}{\sqrt{N}} \sum_j \hat{a}_j \exp(ik\ell j).$$

Here, $\omega_f' = \omega_f - \delta_1$, $\delta_1 = \omega_{fb} - \omega_0$ is detuning between the quantized mode and the transition frequency ω_{fb} , and $\delta_2 = \omega_{fc} - \Omega$ is detuning between the classical field and the transition frequency ω_{fc} . The original band structure is characterized by the dispersion relation

$$\Omega_k = \delta_2 - \delta_1 + 2J \cos(k\ell). \quad (10)$$

Obviously, the photonic band is centered at $k = \pi/(2\ell)$.

To enhance the coupling strength between the probe field and atoms, we can dope more, say N_A , identical noninteracting three-level Λ -type atoms in each cavity. In this case, the system Hamiltonian is changed into

$$H = H_C + \sum_j (H_A^j + H_{CA}^j),$$

with

$$H_A^j = \omega_f s_{ff}^j + \omega_b s_{bb}^j + \omega_c s_{cc}^j, \quad (11)$$

$$H_{CA}^j = g_1 s_{fb}^j a_j + g_2 e^{-i\Omega t} s_{fc}^j + \text{H.c.}, \quad (12)$$

where, in each cavity,

$$s_{\alpha\beta}^j = \sum_l \sigma_{\alpha\beta j}^l. \quad (13)$$

denote the collective dipole between $|\alpha\rangle$ and $|\beta\rangle$ for $\alpha \neq \beta$.

For each cavity, the collective effect of doped three-level atoms can be described by quasi-spin-wave boson operators

$$A_j = \frac{s_{bf}^j}{\sqrt{N_A}}, \quad C_j = \frac{s_{bc}^j}{\sqrt{N_A}}, \quad (14)$$

which create two collective states $|1_c\rangle_j = C_j^\dagger |\nu\rangle$ and $|1_f\rangle_j = A_j^\dagger |\nu\rangle$ with one quasiparticle excitation. Here $|\nu\rangle = |b_1, b_2, \dots, b_{N_A}\rangle$ is the collective ground state with all N_A atoms staying in the ground state $|b\rangle$. In low excitation and large N_A limit, the two quasi-spin-wave excitations behave as two bosons [26], and they satisfy the bosonic commutation relations

$$[A_j, A_j^\dagger] = 1, \quad [C_j, C_j^\dagger] = 1, \quad (15)$$

and $[A_j, C_j] = 0$. The commutation relations between A_j and C_j means that, in each cavity, the two quasispin wave generated by N_A three-level Λ -type atoms are independent of each other.

In the interaction picture with respect to

$$H_0 = \omega_0 \sum_j a_j^\dagger a_j + \sum_j [\omega_f s_{ff}^j + \omega_b s_{bb}^j + \omega_c s_{cc}^j],$$

and by the Fourier transformations

$$F_k = \sum_j \frac{F_j}{\sqrt{N_A}} e^{ik\ell j} \quad (16)$$

for $F = a, A$, and C *et al.*, the interaction Hamiltonian reads as $V = \sum_k V_k$,

$$V_k = \epsilon_k a_k^\dagger a_k + \delta_2 A_k^\dagger A_k + G_1 A_k^\dagger a_k + g_2 A_k^\dagger C_k + \text{H.c.}, \quad (17)$$

where

$$\epsilon_k = 2J \cos(k\ell) + \delta_2 - \delta_1 \quad (18)$$

is the dispersion relation of CROW. Here, the effective photonic band-spin wave coupling $G_1 = g_1 \sqrt{N_A}$ is $\sqrt{N_A}$ times enhancement of g_1 and thus result in a strong coupling.

We also notice that the SU(2) algebra defined by the quasispin operators T_- , T_+ and T_3 in the coordinate space can also be realized in the momentum space through the Fourier transformations as

$$(T_-)_k = A_k^\dagger C_k, \quad (T_+)_k = C_k^\dagger A_k, \quad (T_3)_k = \frac{1}{2}(C_k^\dagger C_k - A_k^\dagger A_k). \quad (19)$$

This means the interaction Hamiltonian possesses an intrinsic dynamic symmetry described by a large algebra containing SU(2) as a subalgebra. Technologically this observation will help us to diagonalize the Hamiltonian Eq. (17) as follows.

IV. DRESSED COLLECTIVE STATES: POLARITONS

In each cavity the strong couplings will coherently mix the photon and the artificial atoms to form dressed states. The collective effect of these dressed states can make the collective excitations, which behave as bosons (called polaritons) in the low excitation limit. Mathematically we write the boson operator a_k , A_k , and C_k as an operator-valued vector

$$\vec{b}_k = \begin{pmatrix} a_k \\ A_k \\ C_k \end{pmatrix}.$$

In terms of those operator-valued vectors $\{\vec{b}_k\}$, the interaction Hamiltonian V_k can be rewritten as

$$V_k = \vec{b}_k^\dagger M \vec{b}_k,$$

where

$$M = \begin{bmatrix} \epsilon_k & G_1 & 0 \\ G_1 & \delta_2 & g_2 \\ 0 & g_2 & 0 \end{bmatrix}.$$

Now we solve the eigenvalue problem of the matrix M . Then V_k can be diagonalized to construct the polariton operators, which are described by the linear combination of the quantized electromagnetic field operators and the atomic collective excitation operator of quasispin waves. The three real eigenvalues of M

$$\lambda_k^{[1]} = \beta_+^{[k]} + \beta_-^{[k]} + \frac{1}{3}(\epsilon_k + \delta_2),$$

$$\lambda_k^{[2]} = \kappa \beta_+^{[k]} + \kappa^2 \beta_-^{[k]} + \frac{1}{3}(\epsilon_k + \delta_2),$$

$$\lambda_k^{[3]} = \kappa^2 \beta_+^{[k]} + \kappa \beta_-^{[k]} + \frac{1}{3}(\epsilon_k + \delta_2), \quad (20)$$

are written in terms of $\kappa = (-1 + i\sqrt{3})/2$ and

$$\beta_\pm^{[k]} = \sqrt[3]{-\frac{q}{2} \pm \sqrt{\left(\frac{q}{2}\right)^2 + \left(\frac{p}{3}\right)^3}},$$

$$p = -\frac{1}{3}\epsilon_k^2 + \frac{1}{3}\delta_2\epsilon_k - G_1^2 - g_2^2 - \frac{1}{3}\delta_2^2,$$

$$q = \frac{1}{27} [3\delta_2\epsilon_k^2 - 2\epsilon_k^3 + (18g_2^2 - 9G_1^2 + 3\delta_2^2)\epsilon_k - 2\delta_2^3 - 9G_1^2\delta_2 - 9g_2^2\delta_2].$$

For a nonzero eigenvalue $\lambda_k^{[i]}$, the polariton operators can be defined as

$$P_k^{[i]} = \frac{1}{r_i} \left[\frac{G_1}{\lambda_k^{[i]} - \epsilon_k} a_k + A_k + \frac{g_2}{\lambda_k^{[i]}} C_k \right], \quad (21)$$

where

$$r_i = \sqrt{\frac{|G_1|^2}{|\lambda_k^{[i]} - \epsilon_k|^2} + 1 + \frac{|g_2|^2}{|\lambda_k^{[i]}|^2}}. \quad (22)$$

When the detunings approximately satisfy the resonance transition condition so that $\epsilon_k=0$ for some k , the dark-state polariton can be constructed as an eigenstate with vanishing eigenvalue. For concreteness, we first consider the case with the detuning $\delta_2=\delta_1=0$, which means that the probe light and the classical field are resonant with the Λ -type atoms in each cavity. The polariton operators at the band center $k=k_0 = \pi/(2\ell)$ can be constructed as

$$P_{k_0}^{[1]} = \frac{1}{\sqrt{2}}(A_{k_0} - B_{k_0}), \quad (23a)$$

$$P_{k_0}^{[2]} = a_{k_0} \cos \theta - C_{k_0} \sin \theta, \quad (23b)$$

$$P_{k_0}^{[3]} = \frac{1}{\sqrt{2}}(A_{k_0} + B_{k_0}), \quad (23c)$$

with $\tan \theta = G_1/g_2$, and

$$B_{k_0} = a_{k_0} \cos \theta + C_{k_0} \sin \theta. \quad (24)$$

Here, $P_{k_0}^{[2]}$ is the dark-state polariton (DSP), which traps the electromagnetic radiation from the excited state due to quantum interference canceling; B_{k_0} is called the bright-state polariton [26].

For another case, we assume that, in each cavity, the frequency of the probe light ω_0 has a nonzero detuning from the transition frequency ω_{ab} , i.e., $\delta_1 = \Delta \neq 0$. By adjusting the frequency of the classical field, $\delta_2 = \Delta$ can be realized, and then the condition $\epsilon_k=0$ is satisfied at the band center. So the dark-state polariton exists. With the polariton operators

$$Q_{k_0}^{[1]} = \xi \left[G_1 a_{k_0} + \frac{\Delta - \alpha}{2} A_{k_0} + g_2 C_{k_0} \right], \quad (25a)$$

$$Q_{k_0}^{[2]} = a_{k_0} \cos \theta - C_{k_0} \sin \theta, \quad (25b)$$

$$Q_{k_0}^{[3]} = \xi \left[G_1 a_{k_0} + \frac{\Delta + \alpha}{2} A_{k_0} + g_2 C_{k_0} \right], \quad (25c)$$

for

$$\xi = \sqrt{2/(\alpha - \Delta)\alpha},$$

the interaction Hamiltonian V_{k_0} is diagonalized. Here,

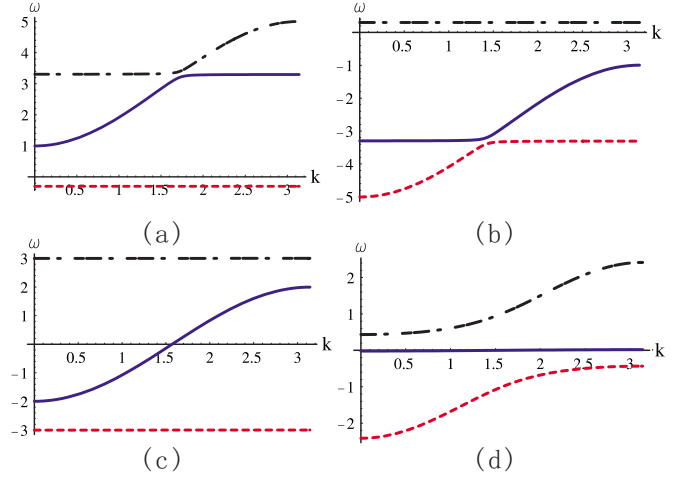


FIG. 3. (Color online) The band structure at the first excitation space. Here the eigenfrequency is plotted as a function of the wave vector k . We have set $J=-1$. The other parameters are set as follows: $\delta_1=0$, (a) $\delta_2=3|J|$, $G_1=0.1J$, $g_2=1.0|J|$. (b) $\delta_2=-3|J|$, $G_1=0.1J$, $g_2=1.0|J|$. (c) $\delta_2=0$, $G_1=0.1|J|$, $g_2=3|J|$. (d) $\delta_2=0$, $G_1=|J|$, $g_2=0.1|J|$. The wave vector k is in units of $1/\ell$.

$$\alpha = \sqrt{\Delta^2 + 4G_1^2 + 4g_2^2}, \quad (26)$$

the DSP $Q_{k_0}^{[2]}$ is the specific light-matter dressed states, which particularly appears in EIT.

Actually, for a probe light with nonzero detuning δ_1 and small band around $k=k_1$ ($k_1 \neq k_0$), by adjusting the detuning δ_2 to satisfy $\epsilon_{k_1}=0$, at the model $k=k_1$, we can also construct the polariton operators similar to those of Eq. (25) with δ_2 replacing Δ and k_1 replacing k_0 .

V. BAND STRUCTURE OF POLARITONS

From the above discussion, it can be observed that the spectra of the hybrid system consists of three bands, and there exists gaps among these three bands for a nonvanishing G_1 and g_2 . Since the number of total excitations

$$N_k = a_k^\dagger a_k + A_k^\dagger A_k + C_k^\dagger C_k \quad (27)$$

commutes with V_k , the number of excitation N_k is conserved, while the numbers $a_k^\dagger a_k$, $A_k^\dagger A_k$, and $C_k^\dagger C_k$ of different type excitations are mutually convertible by adjusting some parameters. In Fig. 3 we plot the eigenfrequencies as a function of the wave vector k in the one excitation subspace. It can be seen from Figs. 3(a) and 3(b) that the bandwidth can be tuned by adjusting the detuning δ_2 and the coupling strength g_2 . For a fixed coupling strength g_2 , when $\delta_2 \ll -|g_2|$, the lowest band (the red dashed line) has a large bandwidth, which ensures the accommodation of the bandwidth of the entire pulse; when $\delta_2 \gg |g_2|$, the bandwidth of the lowest band $W_0 \approx 0$. Hence, for a light pulse that is a superposition of many k states, its distribution in the k space can be entirely contained in the photonic band of the CROW by setting $\delta_2 \ll -|g_2|$. By adiabatically tuning the detuning from $\delta_2 \ll -|g_2|$ to $\delta_2 \gg |g_2|$, the light pulse can be stopped. Such an approach to stopping light with an all-optical process has

been investigated theoretically by numerical simulations [7–9] and a similar all-optical scheme has already been realized in a recent experiment [5].

When the light pulse enters the medium, photons and atoms combine to form excitations known as polaritons. Because the spin wave propagates together with the light pulse inside the medium, the group velocity of the light pulse is reduced by a large order of magnitude. Thus, by analyzing the contribution of photons to the polaritons, it can be well understood that the group velocity of the probe field is stopped and revived. For the sake of simplicity, firstly, we focus on the polaritons at the band center and consider the situation with the resonance transition. The operators of polaritons are the linear combination of that of photons and atoms with the following form:

$$P_{k_0}^{[1]} = \frac{1}{\sqrt{2}}(A_{k_0} - a_{k_0} \cos \theta - C_{k_0} \sin \theta), \quad (28a)$$

$$P_{k_0}^{[2]} = a_{k_0} \cos \theta - C_{k_0} \sin \theta, \quad (28b)$$

$$P_{k_0}^{[3]} = \frac{1}{\sqrt{2}}(A_{k_0} + a_{k_0} \cos \theta + C_{k_0} \sin \theta), \quad (28c)$$

where

$$\cos \theta = \frac{g_2}{\sqrt{g_2^2 + G_1^2}}, \quad (29)$$

$$\sin \theta = \frac{G_1}{\sqrt{g_2^2 + G_1^2}}. \quad (30)$$

The contribution of photons to dark polaritons can be explicitly analyzed. It can be obtained that the dark polariton appears like photons with probability approximately to one when $g_2 \gg G_1$, that is, $P_{k_0}^{[2]} \approx a_{k_0}$. Thus, if we initially set $g_2 \gg G_1$, this means the middle band can accommodate many components of the input pulse. It is easy to find that when $g_2 \ll G_1$, the contribution of photons in the polariton becomes purely atomic; that is, $P_{k_0}^{[2]} \approx C_{k_0}$. Thus, when the pulse is completely in the system, the adiabatical performance changes the dark polariton from photons to atoms and vice versa. A similar situation can be found at the second band under the two-photon resonance from Eq. (25).

In order to give a general argument, we plot the coefficients before a_k , A_k , and C_k in the polaritons as functions of the momentum index k , respectively, in Fig. 4. For the convenience of expression, we denote $d_{jk}^{[i]}$ ($j=1, 2, 3$) as the coefficients before the operators a_k , A_k , and C_k for different eigenvalues $i=1, 2, 3$, respectively. From Eq. (21), the expression of $d_{jk}^{[i]}$ can be obtained as follows:

$$d_{1k}^{[i]} = \frac{1}{r_i} \frac{G_1}{\lambda_k^{[i]} - \epsilon_k},$$

$$d_{2k}^{[i]} = \frac{1}{r_i},$$

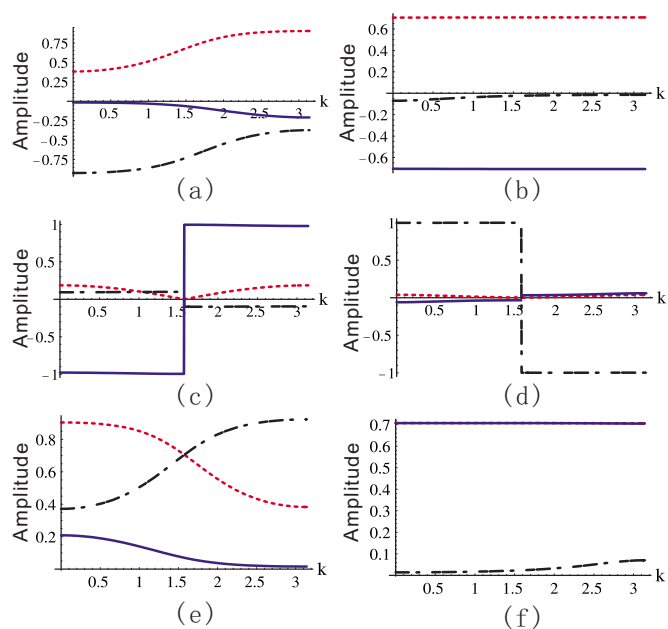


FIG. 4. (Color online) The contribution of photons and two spin waves in the polaritons d_{jk} as functions of k for the first eigenfrequency $\lambda_k^{[1]}$ (a) and (b); the second eigenfrequency $\lambda_k^{[2]}$ (c) and (d), and the third eigenfrequency $\lambda_k^{[3]}$ (e) and (f). $\delta_1 = \delta_2 = 0$, $J = -1$. For (a), (c), and (e), we set $G_1 = |J|$ and $g_2 = 0.1|J|$. For (b), (d), and (f), we set $G_1 = 0.1|J|$ and $g_2 = 3|J|$. The wave vector k is in unit of $1/\ell$.

$$d_{3k}^{[i]} = \frac{1}{r_i} \frac{g_2}{\lambda_k^{[i]}}. \quad (31)$$

In each figure, the red dashed line represents the magnitude $d_{2k}^{[i]}$ of spin waves generated by the atomic transition between $|b\rangle$ and $|f\rangle$; the blue solid line denotes the amplitude $d_{3k}^{[i]}$ of spin waves between $|b\rangle$ and $|c\rangle$; and the black dash-dotted line describes the magnitude $d_{1k}^{[i]}$ of the photonic component. It can be observed that for the incident pulse with momentum distribution around $k = \pi/(2\ell)$, photons make a larger contribution to the polaritons at $G_1 \gg g_2$ than at the condition $G_1 \ll g_2$. The contribution of photons in the polariton of the second band, shown in Figs. 4(c) and 4(d), is modified completely by the coupling strength of light and matter: spin waves C_k take large proportions when $G_1 \gg g_2$ and photons a_k have large contributions when $G_1 \ll g_2$. Hence, the second band can be used to convert the quantum information originally carried by photons into long-lived spin states of atoms.

The characteristic of our hybrid system is that the “dark state” can be realized in a straightforward way. This gives rise to quasiparticles—the dark polariton, which reflects the crucial idea of the EIT—the coherent population trapping for the quantized probe field. Actually, a DSP is an atomic collective excitation (quasispin wave) dressed by the quantized probe light. This point can be seen directly from Eq. (25b). The contributions of light or atoms in DSP can be varied by adapting the amplitude of the classical field, which has been discussed in the last paragraph. Thus, in our hybrid system, the DSP offers a possible control scheme for slowing light. This accessible scheme can be observed from the change of

bandwidth. In Figs. 3(c) and 3(d), we plot the eigenfrequency as a function of the wave vector k in the first excitation space for a given δ_2 . It shows that, when $g_2 \gg G_1$, the bandwidth of the middle band (the blue solid line) has a large bandwidth; when $g_2 \ll G_1$, the bandwidth of the middle are approximately to zero. The couplings also make the center of bands away from ω_0 , ω_{ab} , and ω_{cb} , respectively. This fact means that by tuning the coupling strength from $g_2 \gg G_1$ to $g_2 \ll G_1$ adiabatically, we can stop the input light pulse and then reemit it. Thus, via selecting a classical field with a suitable frequency, the quantum state of an input pulse can be converted into the doped three-level atoms simply by switching off the driving field, and then by turning on the driving field, the stored information can be retrieved.

To give a concrete example, we consider the resonant transition with $\delta_1 = \delta_2 = 0$. In this case, the corresponding group velocities at each band center are

$$v_g^1[k_0] = \frac{G_1^2}{G_1^2 + g_2^2} J \ell, \quad (32)$$

$$v_g^2[k_0] = \frac{2g_2^2}{G_1^2 + g_2^2} J \ell, \quad (33)$$

$$v_g^3[k_0] = \frac{G_1^2}{G_1^2 + g_2^2} J \ell. \quad (34)$$

It can be seen that, at the band center, when $g_2 \gg G_1$, the lowest band [the red dashed line in Figs. 3(c) and 3(d)] and the highest band [the black dash-dotted line in Figs. 3(c) and 3(d)] exhibit zero group velocity and zero bandwidth, but the middle band [the blue solid one in Figs. 3(c) and 3(d)] exhibits a large group velocity and a large bandwidth; in reverse, when $g_2 \ll G_1$, the middle band exhibits zero group velocity and vanishing bandwidth, but the lowest band and the highest band exhibit large group velocities and large bandwidths. Hence, in this system, focusing on the middle band, a light pulse can be stopped by the following process: Initially setting $g_2 \gg G_1$, the middle band accommodates the entire pulse. After the pulse is completely in this system, we vary the coupling strength until $g_2 \ll G_1$ adiabatically. The lowest band also can be used to stop light by tuning g_2 from $g_2 \ll G_1$ to $g_2 \gg G_1$.

Finally, we give some estimation about the group velocity according to the realistic parameters, which are taken for the array of coupled toroidal microcavities [12,22]. The distance ℓ between the microcavities is $15.69 \mu\text{m}$ [5], and the evanescent coupling between the cavities is $J = 1.1 \times 10^7 \text{ s}^{-1}$. Within each cavity, the coupling strength between the atom and the quantum fields is $g_1 = 2.5 \times 10^9 \text{ s}^{-1}$, and the Rabi frequency is $g_2 = 7.9 \times 10^{10} \text{ s}^{-1}$. When $N = 10\,000$ atoms are contained in each cavity, the group velocity of light at the second band center is estimated at 31 m/s .

VI. SUSCEPTIBILITY ANALYSIS FOR LIGHT PROPAGATION IN THE DOPED CROW

When a light beam incidents on an optically active medium, the medium will give a response to the control light.

Usually, the index of refraction can reach high values near a transition resonance, but the high dispersion always accompanies a high absorption in the resonance point. In EIT, the resonant transition or the two-photon resonance renders a medium transparent over a narrow spectral range within the absorption line. Also in this transparent window, the rapidly varying dispersion is created, which leads to very slow group velocity and zero group velocity. In this section, we will investigate the dispersion and the absorption property of the gapped light in our hybrid system. We use the dynamic algebraic method developed for the atomic ensemble based quantum memory with EIT [26,27].

We begin with the Hamiltonian (17) in the k -space representation. When the atomic decay is considered, we write down the Heisenberg equations of operators a_k , A_k , and C_k for each mode k ,

$$\partial_t a_k = -(\gamma + i\epsilon_k) a_k - iG_1 A_k, \quad (35)$$

$$\partial_t A_k = -(\gamma_A + i\delta_2) A_k - iG_1 a_k - ig_2 C_k, \quad (36)$$

$$\partial_t C_k = -\gamma_C C_k - ig_2 A_k, \quad (37)$$

where we have phenomenologically introduced the damping rate of cavity γ , and the decay rate γ_A , γ_C of the energy levels $|f\rangle$ and $|c\rangle$ of the three-level system, respectively. We also assume that

$$\gamma_A \gg \gamma_C \gg \gamma.$$

To find the steady-state solution for the above motion equations, it is convenient to remove the fast varying part of the light field and the atomic collective excitations by making a transformation

$$F_k = \tilde{F}_k e^{-i\epsilon_k t} \quad (38)$$

for $F_k = a_k$, A_k , and C_k . For the convenience of notation, we drop the tilde, and then the above Heisenberg equations become

$$\partial_t C_k = (i\epsilon_k - \gamma_C) C_k - ig_2 A_k,$$

$$\partial_t A_k = [i(\omega_k - \delta_1) - \gamma_A] A_k - iG_1 a_k - ig_2 C_k, \quad (39)$$

where $\omega_k = 2J \cos(k\ell)$.

The electric field of the quantized probe light with k -space representation

$$E_k(t) = \sqrt{\frac{\omega_0}{2V\epsilon_0}} a_k e^{-i\epsilon_k t} + \text{H.c.} \quad (40)$$

results in a linear response of medium, which is described by the polarization

$$\langle P_k \rangle = \langle p_k \rangle \exp(-i\epsilon_k t) + \text{H.c.}$$

Here,

$$\langle p_k \rangle = \frac{\mu}{V} \sqrt{N_A} \langle A_k \rangle \quad (41)$$

is a slowly varying complex polarization determined by the population distribution on $|f\rangle$ and $|c\rangle$; μ denotes the dipole

moment between $|f\rangle$ and $|c\rangle$, and V is the effective mode volume [28]. It is also related to the susceptibility χ_k of the k space by

$$\langle p_k \rangle = \epsilon_0 \chi_k \sqrt{\frac{\omega_0}{2V\epsilon_0}} \langle a_k \rangle. \quad (42)$$

The real part χ_k^r and imaginary part χ_k^i of the susceptibility correspond to the dispersion and absorption, respectively.

In order to calculate the susceptibility, we first find the steady-state solution by letting $\partial_t A_k = 0$ and $\partial_t C_k = 0$ in Eq. (39). The expectation value of A_k over a stable state is explicitly obtained as

$$\langle A_k \rangle = \frac{iG_1[i(\omega_k + \delta) - \gamma_C]}{[i(\omega_k - \delta_1) - \gamma_A][i(\omega_k + \delta) - \gamma_C] + g_2^2} \langle a_k \rangle, \quad (43)$$

where $\delta = \delta_2 - \delta_1$. Since the coupling coefficient

$$g_1 = -\mu \sqrt{\frac{\omega_0}{2V\epsilon_0}},$$

the real part χ_k^r and imaginary part χ_k^i of the linear complex susceptibility χ_k are obtained as

$$\begin{aligned} \chi_k^r &= F[\epsilon_k g_2^2 - (\epsilon_k - \delta_1)(\gamma_C^2 + \epsilon_k^2)]L(k), \\ \chi_k^i &= F[\epsilon_k^2 \gamma_A + (\gamma_A \gamma_C + g_2^2)\gamma_C]L(k), \end{aligned} \quad (44)$$

where

$$L(k)^{-1} = [\gamma_A \gamma_C + g_2^2 - \epsilon_k(\epsilon_k - \delta_2)]^2 + [\epsilon_k \gamma_A + (\epsilon_k - \delta_2)\gamma_C]^2, \quad (45)$$

and $F = 2G_1^2 / \omega_0$.

Since the susceptibility depends on k , in Fig. 5 the real and imaginary susceptibilities χ_k^r , χ_k^i are plotted versus the detuning difference $\delta = \delta_2 - \delta_1$ in units of γ_A ($\gamma_A = 10^3 \gamma_C$), where we assume that the central frequency of light pulse is at $k = \pi/4\ell$.

It is observed that, when the detuning δ_1, δ_2 satisfy $\epsilon_k = 0$, that is, the two-photon resonance is satisfied, both the real and imaginary susceptibilities vanish, the absorption is absent, and the index of refraction is unity. Thus the whole system becomes transparent under the driving of the strong classical control field. Through Eq. (18), we obtain that the momentum index k together with the nearest-neighbor evanescent coupling strength J determine the range where the transparency window occurs. The width of the transparency window depends on the control field Rabi frequency g_2 , which is shown by comparing Figs. 5(a) and 5(b).

Finally, to consider the role of the intercavity coupling J , we plot the real (solid line) and the imaginary (dashed line) part of the susceptibility as a function of the intercavity coupling strength J , shown in Fig. 6. It can be observed that when the incident pulse is center at $k = \pi/(2\ell)$, the susceptibility is independent of J [see Fig. 6(f)]; for the input pulse centered at $k = \pi/(4\ell)$, in the vicinity of a frequency corresponding to the two-photon Raman resonances, the medium made of atoms becomes transparency with respect to the input pulse within the photonic band. By comparing Figs. 6(a) and 6(b), it can be found that the detuning difference δ de-

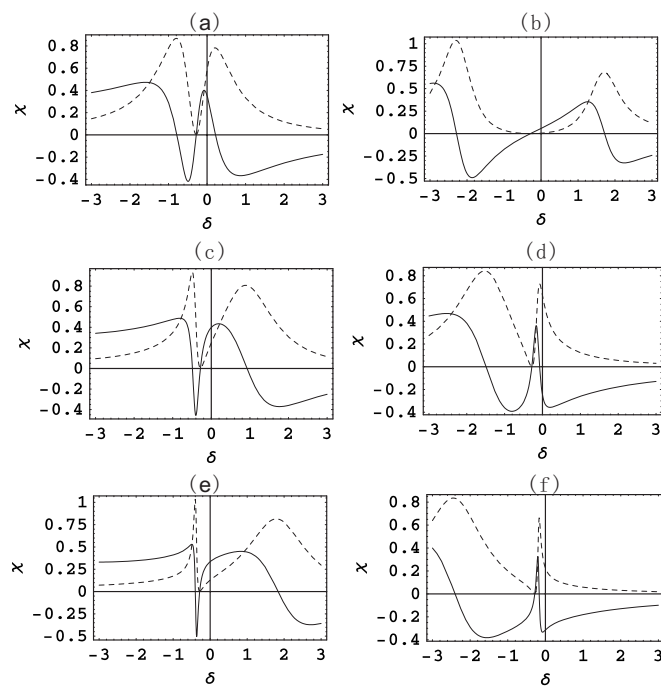


FIG. 5. Real (solid) and imaginary (dotted) parts of the linear susceptibility as a function of normalized detuning δ at $k = \pi/4$. The parameters are set as $G_1 = 1$, $J = 0.2$, $\ell = 1$. (a) $g_2 = 0.5$, $\delta_2 = 0$; (b) $g_2 = 2$, $\delta_2 = 0$; (c) $g_2 = 0.5$, $\delta_2 = 1$; (d) $g_2 = 0.5$, $\delta_2 = -1$; (e) $g_2 = 0.5$, $\delta_2 = 2$; (f) $g_2 = 0.5$, $\delta_2 = -2$. δ is in units of $\gamma_A = 1$.

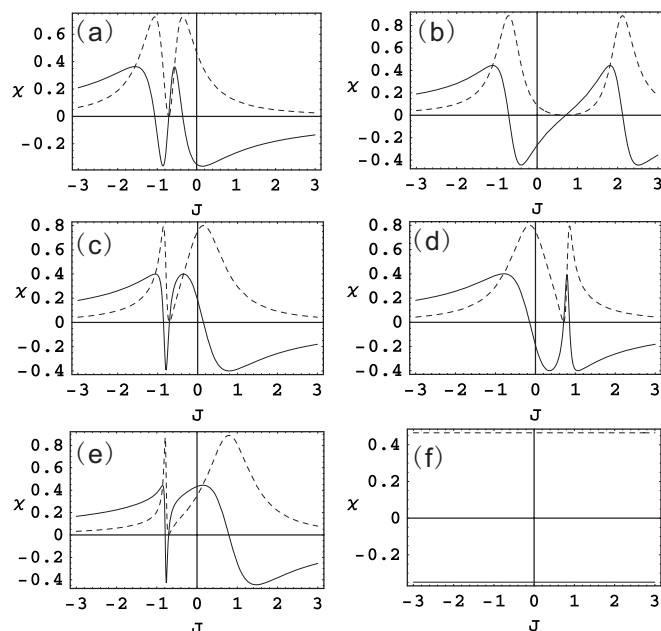


FIG. 6. Real (solid) and imaginary (dotted) parts of the linear susceptibility as a function of the intercavity coupling strength J . The parameters are set as $G_1 = 1$, $\ell = 1$. (a) $g_2 = 0.5$, $\delta_2 = 0$, $\delta = 1$, and $k = \pi/4$; (b) $g_2 = 2$, $\delta_2 = 0$, $\delta = -1$, and $k = \pi/4$; (c) $g_2 = 0.5$, $\delta_2 = 1$, $\delta = 1$, and $k = \pi/4$; (d) $g_2 = 0.5$, $\delta_2 = -1$, $\delta = -1$, and $k = \pi/4$; (e) $g_2 = 0.5$, $\delta_2 = 2$, $\delta = 1$, and $k = \pi/4$; (f) $g_2 = 0.5$, $\delta_2 = 0$, $\delta = 1$, and $k = \pi/2$. J is in units of $\gamma_A = 1$.

termines the position where the transparency window occurs, and the intensity of the control beam decides the width of the transparency window; it can also be observed from Figs. 5 and 6 that the larger the detuning $|\delta_2|$ is, the broader transparency window the spectra of this system has.

VII. CONCLUSION AND REMARKS

We have studied a hybrid system, which consists of N homogeneously coupled resonators with three-level Λ -type atoms doped in each cavity. The electromagnetically induced transparency (EIT) effect can enhance the ability for coherent manipulations on the photon propagation in the CROW, namely, the photon transmission along the CROW can be well controlled by the amplitude of the driving field. With these results, it is expected that the quantum information encoded in the input pulse can be stored and retrieved by adiabatically tuning g_2 from $g_2 \ll G_1$ to $g_2 \gg G_1$.

Also it can be seen that our hybrid architecture possesses more controllable parameters for transferring photons in an array of coupled cavities: two coupling strength g_1, g_2 and

two detunings. Typically, in two-photon resonance, the light can be stopped only by controlling the amplitude of the classical field. In comparison with our scheme, the all-optical architecture with the passive optical resonator [7] only has two controllable parameters, the coupling strength between the side-coupled cavity and each of the CROW and the detuning between resonance frequency of side-coupled cavity and that of cavity, which constitute the CROW. On the other hand, the standard EIT approach only uses the single ‘‘cavity’’ and thus there is not a controllable photonic band structure. The on-chip periodic structure used here actually can implement the EIT manipulation for photonic storage in the periodic lattice fixing atoms spatially [26].

ACKNOWLEDGMENTS

This work is supported by the NSFC with Grants Nos. 90203018, No. 10474104 and No. 60433050, and NFRPC with Grant No. 2006CB921206 and NO. 2005CB724508. The author L.Z. gratefully acknowledges the support of K. C. Wong Education Foundation, Hong Kong.

-
- [1] S. E. Harris, *Phys. Today* **50**(7), 36 (1997).
 - [2] M. Fleischhauer and M. D. Lukin, *Phys. Rev. Lett.* **84**, 5094 (2000).
 - [3] L. V. Hau, S. E. Harris, Z. Dutton, and C. H. Beroozzi, *Nature (London)* **397**, 594 (1999).
 - [4] S. E. Harris and L. V. Hau, *Phys. Rev. Lett.* **82**, 4611 (1999).
 - [5] Q. Xu, S. Sandhu, M. L. Povinelli, J. Shakya, S. Fan, and M. Lipson, *Phys. Rev. Lett.* **96**, 123901 (2006).
 - [6] R. W. Boyd and D. J. Gauthier, *Nature (London)* **441**, 701 (2006).
 - [7] M. F. Yanik and S. Fan, *Phys. Rev. Lett.* **92**, 083901 (2004).
 - [8] M. F. Yanik and S. Fan, *Phys. Rev. A* **71**, 013803 (2005).
 - [9] L. Maleki, A. B. Matsko, A. A. Savchenkov, and V. S. Ilchenko, *Opt. Lett.* **29**, 626 (2004).
 - [10] Z. S. Yang, N. H. Kwong, R. Binder, and A. L. Smirl, *J. Opt. Soc. Am. B* **22**, 2144 (2005).
 - [11] D. G. Angelakis, M. F. Santos, and S. Bose, e-print arXiv:quant-ph/0606159.
 - [12] M. J. Hartmann, F. G. S. L. Brandao, and M. B. Plenio, *Nat. Phys.* **2**, 849 (2006).
 - [13] A. D. Greentree, C. Tahan, J. H. Cole, and L. C. L. Hollenberg, *Nat. Phys.* **2**, 856 (2006).
 - [14] L. Zhou, Y. B. Gao, Z. Song, and C. P. Sun, e-print arXiv:cond-mat/0608577.
 - [15] A. Wallraff, D. I. Schuster, A. Blais, L. Frunzio, R.-S. Huang, J. Majer, S. Kumar, S. M. Girvin, and R. J. Schoelkopf, *Nature (London)* **431**, 162 (2004).
 - [16] A. Blais, R.-S. Huang, A. Wallraff, S. M. Girvin, and R. J. Schoelkopf, *Phys. Rev. A* **69**, 062320 (2004).
 - [17] F. M. Hu, L. Zhou, T. Shi, and C. P. Sun, e-print arXiv:quant-ph/0610250, *Phys. Rev. A*. (to be published).
 - [18] G. R. Jin, P. Zhang, Y. X. Liu, and C. P. Sun, *Phys. Rev. B* **68**, 134301 (2003).
 - [19] J. B. Khurgin, *J. Opt. Soc. Am. B* **22**, 1062 (2005).
 - [20] N. Stefanou and A. Modinos, *Phys. Rev. B* **57**, 12127 (1998).
 - [21] M. Bayindir, B. Temelkuran, and E. Ozbay, *Phys. Rev. Lett.* **84**, 2140 (2000).
 - [22] S. M. Spillane, T. J. Kippenberg, K. J. Vahala, K. W. Goh, E. Wilcut, and H. J. Kimble, *Phys. Rev. A* **71**, 013817 (2005).
 - [23] Z. Song, P. Zhang, T. Shi, and C. P. Sun, *Phys. Rev. B* **71**, 205314 (2005).
 - [24] S. H. Autler and C. H. Townes, *Phys. Rev.* **100**, 703 (1955).
 - [25] U. Fano, *Phys. Rev.* **124**, 1866 (1961).
 - [26] C. P. Sun, Y. Li, and X. F. Liu, *Phys. Rev. Lett.* **91**, 147903 (2003).
 - [27] Y. Li, and C. P. Sun, *Phys. Rev. A* **69**, 051802(R) (2004).
 - [28] M. O. Scully and M. S. Zubairy, *Quantum Optics* (Cambridge University Press, Cambridge, 1997).